sustainability

MDPI

Article

Development of Climate-Based Index for Hydrologic Hazard Susceptibility

Mohamed Salem Nashwan [1,2], Shamsuddin Shahid [2], Eun-Sung Chung [3,*], Kamal Ahmed [2,4] and Young Hoon Song [3]

1 Faculty of Engineering and Technology, Arab Academy for Science, Technology and Maritime Transport (AASTMT), Cairo, 2033 Elhorria, Egypt; m.salem@aast.edu
2 Faculty of Civil Engineering, Universiti Teknologi Malaysia (UTM), Johor Bahru 81310, Malaysia; sshahid@utm.my (S.S.); kamal_brc@hotmail.com (K.A.)
3 Faculty of Civil Engineering, Seoul National University of Science and Technology, 232 Gongneung-ro, Nowon-gu, Seoul 01811, Korea; thddudgns200@naver.com
4 Faculty of Water Resources Management, Lasbela University of Agriculture, Water and Marine Sciences, Uthal, Balochistan 90150, Pakistan
* Correspondence: eschung@seoultech.ac.kr; Tel.: +82-2-970-9017

Received: 27 March 2018; Accepted: 21 June 2018; Published: 26 June 2018

Abstract: An index has been developed for the assessment of geographical distribution of susceptibility to hydrological hazards using easily available climate data. Catastrophe fuzzy theory and data clustering methods were used to avoid subjectivity in the estimation of the index of multiple climate indicators. The proposed index was used for the estimation of geographical distribution of hydrological hazard susceptibility index (HHSI) in Peninsular Malaysia using gauge-based, gridded rainfall and temperature data for the period 1948–2010. The results showed that the northeast regions of Peninsular Malaysia are more susceptible to hydrological hazard, which matches very well with the general conception of the hydrological hazard susceptible zones. Assessment of susceptibility for sliding different 30-year periods between 1950 and 2010 revealed that HHSI has increased in the south and decreased in the northeast of the peninsula. The decrease in temporal and spatial variability of rainfall in the northeast and the increase in other parts can become the causes of spatial changes in hazard susceptibility. The changes of HHSI in recent years compared to the base period revealed the increase of hazard susceptibility in the south in the range of 8.81% to 21.01%, while a significant decrease (>−31.84%) was observed in the northeast.

Keywords: hydrological hazard susceptibility index (HHSI), Hydrological hazards; Fuzzy catastrophe theory; rainfall variability; aridity

1. Introduction

Susceptibility is a major component of vulnerability, which is defined as the sensitivity to hazards [1]. The susceptibility to hydrological hazards can be broadly defined as the possibility of experiencing water-related challenges, such as water shortage, floods, droughts, etc. It is often considered as a determinant of physical feasibility of business or structural projects, disaster risk insurance premiums, financial cost, etc. A number of studies have indicated that the occurrence of hydrological hazards reduces agricultural productivity [2], property value [3], household income and economic growth [4], and increases the structural development cost [5]. Kauko et al. [6] reviewed the empirical literature and found an extremely negative effect of flooding and droughts on property value. Shahid et al. [5] found that probability of floods has reduced the property price from 10% to 30% in some parts of peninsular Malaysia in the recent years. Brown et al. [4] found that the climate has

significant negative effects on household income, agricultural productivity and economic growth in Sub-Saharan Africa. The probability of hydrological hazards increases structural development cost as more attention is required to design features and protection measures from water risk [5]. These studies indicate that susceptibility to hydrological hazards has a wide range of social and economic impacts.

Different physical, social, economic and environmental factors or processes determine the susceptibility. Climate is a major physical factor that defines the susceptibility to hydrological hazards. The hydrological hazards are higher for the region that has less reliable, sporadically distributed and seasonally concentrated rainfall. Therefore, climatic variables can be used as critical indicators to measure susceptibility to hydrological hazards. Numerous indices have been developed to assess water poverty, water stress, water sustainability and water-related risk using a combination of various physical, environmental, social, economic and policy indicators [7–9]. In most of the indices, one or more climatic indicator has been used to estimate water sustainability as it is well recognized as an important factor for defining water availability, sustainability, and hydrological hazards. A wide range of literature is available where different factors related to climate such as rainfall amount, variability, temperature, etc. have been used as indicators of water sustainability [10], surface availability [11], etc. These studies recognize the importance of various climatic factors in defining water sustainability or water-related risk. However, there is no distinct indicator available so far to assess susceptibility to hydrological hazards based solely on climate data. A climate-based index can provide a preliminary impression of condition or changes of susceptibility to hydrological hazards over a large region such as national or regional scale, which can later be further interpreted with existing socio-economic status to understand disaster risk. It can provide knowledge on susceptibility to hydrological hazard for a longer period and, therefore, can be used as an indication of hydro-climatic behavior that can make a region susceptible to various kinds of hydrological hazards such as floods, droughts, water stress, etc.

Generally, a number of indicators are used for the estimation of an index. The influence of each indicator on the index varies from each other. Various subjective weighting methods are available in the literature for estimation of the index from multiple indicators, which include Analytical Hierarchy Process (AHP), Weighted Linear Combination (WLC), Weighted Sum Model (WSM), Weighted Aggregation Method (WAM), TOPSIS, VIKOR etc., [12–15]. The choice of a method normally depends on the efficiency of the method, existence of data and quality of data. All the methods assign weight or preference to indicators based on their importance for the estimation of the index. Generally, the importance of various indicators is assigned by a decision maker which reflects a personal preference for a specific region or purpose, which eventually precludes their application in another region. In order to avoid subjectivity, a number of data-driven and knowledge-driven techniques have been developed such as frequency ratio, weights of evidence, logistic regression, index of entropy, evidential belief functions, catastrophe theory, etc. [16–25]. Among those data-driven models, catastrophe theory-based index methods have attracted the attention of the scientific community due to its efficacy in modeling [26,27]. The catastrophe theory is designed to deal with discontinuous dynamic systems governed by a potential energy-like function which is suitable for decision making based on available data and reducing subjectivity [26,28,29]. A number of recent studies concluded that the catastrophe progression method is a better approach for multi-criteria decision making by avoiding subjectivity considering specific complexity, ambiguity, and uncertainty of decision making [26,30,31]. The major disadvantage of decision making using catastrophe theory is that the influence or weight of indicators depends on the classification of the indicators values. This adds some sort of subjectivity in the decision making. To overcome this challenge, a data clustering approach based on Jenks optimization is proposed in this study for the classification of the values of each indicator.

The objective of the present study is to develop a climate-based water risk index. Simple indicators which can be calculated easily from readily available data for any region are used for this purpose. The catastrophe theory and data clustering methods have been proposed for the calculation of hydrological hazard susceptibility index (HHSI) from climate-based indicators. A case study of HHSI assessment of Peninsular Malaysia is provided. The index is used for the assessment of the

geographical distribution of HHSI and the recent changes in the susceptibility pattern in Peninsular Malaysia. Furthermore, HHSI is also calculated using equal weight for the comparison of the results obtained using catastrophe theory. The index can be used to identify the factors responsible for water-related hazards in order to have a better knowledge of characteristics of hydrological hazards.

2. Case Study Area

The peninsula of Malaysia, covering an area of 130,596 km^2 was selected to show the effectiveness of HHSI developed in this study. Peninsular Malaysia is divided into 13 states and territories as shown in Figure 1. The topography of the region ranges between zero and 2187 m. According to Köppen climate classification, the climate of peninsula Malaysia is classified as a tropical rainforest climate (Af) with uniform high humid hot temperature and moderate rainfall throughout the year. The average annual rainfall in the peninsula ranges between 1933 mm and 3080 mm (Figure 2). The climate of Peninsular Malaysia is dominated by two monsoons, the northeastern monsoon (NEM), from November to March, and the southwest monsoon (SWM), from May to September. The average annual potential evapotranspiration (PET) over the peninsula, estimated using the Thornthwaite equation [32], shows a large variation from 902 mm from the interior of the north to more than 1800 mm around the coast in the northwest, south, and northeast (NE) (Figure 2).

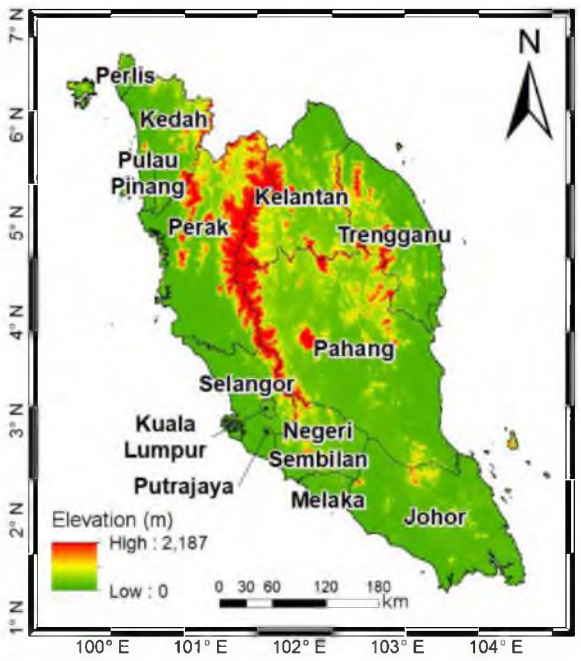

Figure 1. The topography and administrative districts in Peninsular Malaysia.

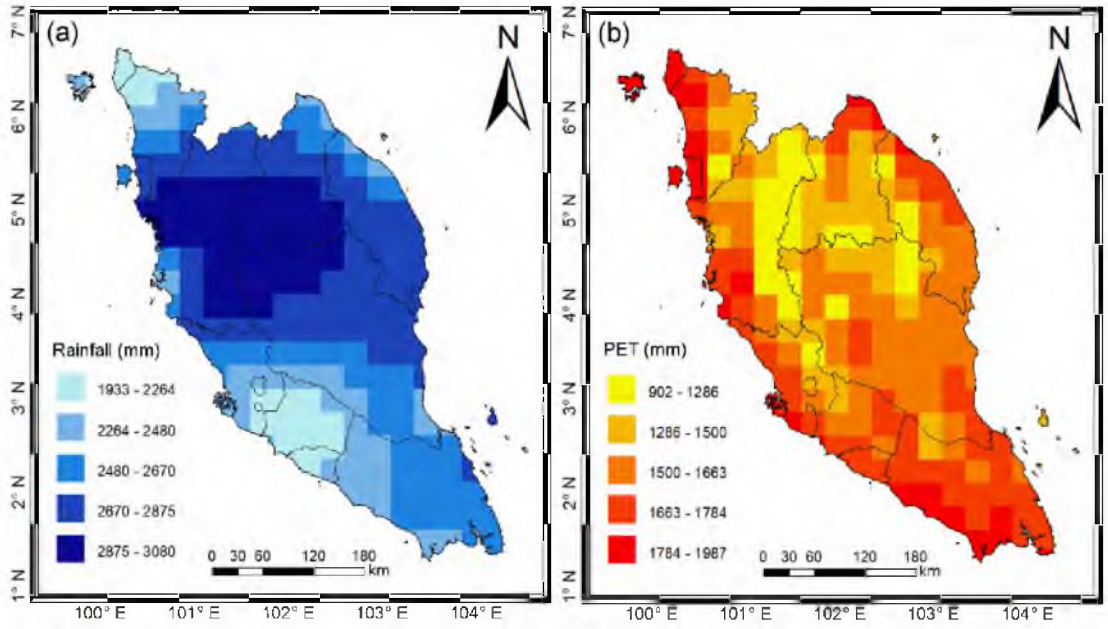

Figure 2. Spatial distribution of (**a**) annual average rainfall; and (**b**) potential evapotranspiration estimated using the Thornthwaite method over Peninsular Malaysia.

3. Data and Methodology

3.1. Data and Sources

Gridded monthly rainfall and temperature data were used in this study for the assessment of susceptibility to hydrological hazards. The major problem often faced in conducting a hydro-climatic study in most parts of the world is the availability of long-term data. Despite availability, uneven distribution and the quality of available data often make it inadequate for the hydrological applications [33]. The gridded data are recommended in the areas where long-term and dense observation data is not available. Thus, in this study, the gridded rainfall and temperature data of the Princeton Global meteorological Forcing Dataset (PGF) developed by Princeton University [34] were used. The rainfall and temperature data at the grid points over Peninsular Malaysia were extracted from the website of PGF [34] for the period 1948–2010.

The PGF data product is developed by merging the reanalysis datasets of the National Centers for Environmental Prediction (NCEP) of National Center for Atmospheric Research (NCAR) and a collection of global observed databases including Climatic Research Unit (CRU) 0.5° gauge-based gridded monthly climate datasets, the Global Precipitation Climatology Project (GPCP) 1.0° gauge-based daily precipitation datasets and the Tropical Rainfall Measuring Mission (TRMM) satellite real-time precipitation datasets [34]. The CRU and GPCP datasets are prepared from a large number of station data distributed over the globe. Smart interpolation technique is used for the interpolation with consideration of topography. Therefore, PGF has been found reliable for hydro-climatic studies in different parts of the world, including Asia [35–39]. One of the major advantages of PGF is its availability at a fine resolution (0.25° × 0.25°) compared to other gridded data and, therefore, it is suitable for the assessment of HHSI at the local scale.

3.2. Methodology

Hydrological Hazard Susceptibility Index (HHSI) was developed and used for the assessment of geographical distribution of HHSI over Peninsular Malaysia using four broad steps: (a) identification of sub-systems; (b) selection and classification of indicators; (c) standardization of data, and (d)

normalization of catastrophe theory; and (e) computation of HHSI. The procedure used in this study is shown by the flowchart in Figure 3. The details of the steps are given in the following sections.

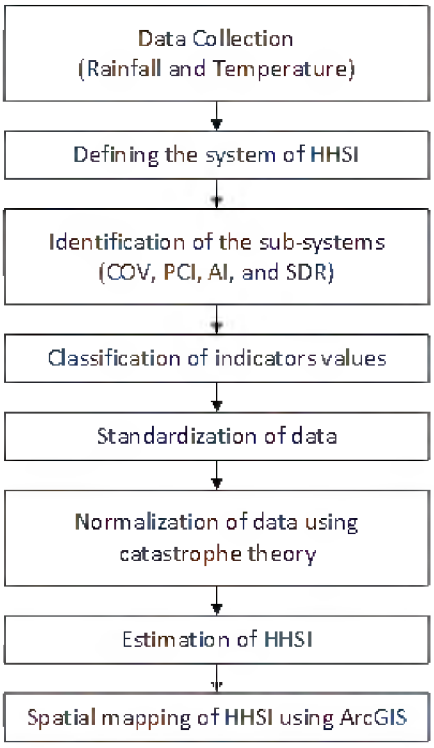

Figure 3. The procedure used in this study for the estimation of HHSI and the preparation of hazard susceptibility map of Peninsular Malaysia.

3.2.1. Identification of Sub-Systems

The concepts and definitions of climate-induced hydrological hazards have been analyzed in many studies [40–42]. Most of the factors identified are based on daily rainfall or temperature such as consecutive wet days, consecutive dry days, one-day maximum rainfall, length of a heat wave, etc. Although these daily data-based indices can provide better information related to hydrological hazards, their use is limited due to a number of reasons: (1) Quality daily rainfall and temperature data are not readily available for a large number of stations in most regions of the World; (2) the presence of outliers, which are very common in daily hydro-climatic data and often mislead to average hydro-climatic condition of a region; and (3) estimation of some daily indices are very complex. Therefore, the indicators which can be estimated from monthly rainfall and temperature data were only considered in this study.

There are many criteria proposed in the literature to select indicators such as availability, measurability, achievability, practicability, necessary skills, relevance, quality, disaggregation, comprehensibility, representation, usability, controllability, responsive, stability, sensitivity, etc. [43–46]. After careful evaluation of different criteria, six criteria were used in this study for the identification of the sub-system and its indicators, (a) availability: The data related to an indicator should be available for existing sources and can be collected easily; (b) measurability: The indicator is measurable in quantitative term; (c) practicality: The indicator can be measured easily with less computation efforts; (d) relevance: The indicator is meaningfully linked to hydrological hazard susceptibility; (e) comprehensibility: The indicator is comprehensible to all and applicable to any region; and (f) sensitivity: The indicator should be responsive to environmental changes.

As a result, the subsystem of the system is defined with four indicators in this study. The justification of selection of the sub-system and the method used for their estimation are discussed below.

Coefficient of Variation of Annual Rainfall

Annual variation of rainfall or coefficient of variation (COV) is considered as one of the most important factors that defines reliability in water resources of a region. A number of studies revealed that annual variability of rainfall is highly correlated to the frequency of floods and droughts [47]. The region having high variability of annual and seasonal rainfall is prone to have more water-related problems than the region where rainfall does not vary significantly from year to year. Therefore, COV of rainfall at a location can be used as an indicator of susceptibility of the location to floods and droughts.

Precipitation Concentration Index

Precipitation Concentration Index (PCI) [48] presents how rainfall is distributed over a water year. It can be estimated using the following equation,

$$\mathrm{PCI} = \frac{\sum_{i=1}^{12} p_i^2}{\left(\sum_{i=1}^{12} p_i\right)^2} \times 100 \tag{1}$$

where p_i is the precipitation of i^{th} month. The PCI is usually high for the region where rainfall is concentrated in a particular season. Most of the annual total rainfall occurs in a few months and the rest of the year is usually dry if the PCI is high [49]. The probabilities of floods and droughts are high for the region where PCI is high compared to the region where PCI is smaller, or rainfall is more or less homogeneously distributed throughout the years. Therefore, PCI at a location can be used as an indicator of susceptibility to flood and droughts of the area.

Aridity Index

Aridity index (AI) has been defined in a number of ways in the literature. However, the UNESCO definition of AI is straightforward and easy to estimate, which is as below,

$$\mathrm{AI} = \frac{R}{\mathrm{PET}} \tag{2}$$

where R is the annual total rainfall and PET is the annual total potential evapotranspiration. The PET can be estimated from monthly mean temperature using Thornthwaite equation [32]:

$$\mathrm{PET} = 16\left(\frac{L}{12}\right)\left(\frac{N}{30}\right)\left(\frac{10T_a}{I}\right)^a \tag{3}$$

where T_a is the monthly average of daily temperature (°C); N is the number of days in the month; L is the average day length (hours) of the month; I is a heat index which depends on the 12 monthly mean temperatures; and a is a constant which depends on the heat index of the month. The AI is high for the region where PET is higher compared to rainfall. Therefore, AI can be used to define water stress or water abundance in an area.

Spatial Variability of Rainfall

The spatial distribution of rainfall (SDR) at a grid point is estimated as the variability of mean rainfall in surrounding locations compared to mean rainfall at the grid point.

$$\mathrm{SDR} = \frac{R_v}{R_i} \tag{4}$$

where R_i is the annual mean rainfall at the grid point i; and R_v is the spatial variability of annual mean rainfall around the station i. It was estimated as the standard deviation of annual mean rainfall of the grid points surrounding the grid point i. Heterogeneous distribution of rainfall can be easily linked to water risk of a region [50]. Concentration of rainfall in a smaller region increases the probability of flood, while precipitation with less quantity leads to water scarcity. Therefore, water scarcity can be noticed at a micro level even in the region where average rainfall is high. This is often noticed in arid and semi-arid regions where rainfall is very erratic and sparsely distributed. Localized flush flood and crop failure due to water scarcity in a topical region is often blamed for high heterogeneity in rainfall distribution. Therefore, SDR can be considered as an indicator of susceptibility to both flush flood and water stress.

3.2.2. Classification of Indicators

The sub-system of the system is defined using indicators. These indicators are specific and provide extensive information on current conditions of multiple hydrological hazards of the study area. The collected indicator data over the study area are decomposed or classified into a number of levels using Jenks optimization method [51]. The classification of the values of an indicator has a significant impact on overall importance or weight of the indicator. It has been found that weight of an indicator changes when values are classified into different ranges. Therefore, subjectivity in estimation of the index using catastrophe theory cannot be completely avoided. In order to overcome this difficulty, a data clustering method known as Jenks optimization [51] was used in this study for the classification of values of each indicator. Jenks method divides data in such a way that variance within each class is minimum but the variance among the mean values of the classes is maximum. The advantage of Jenks classification method is that it identifies the real classes with the data. Another advantage of this classification method is that it was developed with the intention of dividing data into a relatively few data classes. As catastrophe models can handle a maximum of five control variables, Jenks optimization is the best option for classification of data according to the natural variability in order to avoid subjectivity in classification. Finally, the average value of each decomposed or classified data was considered for representing each indicator.

3.2.3. Standardization of Data

The linear standardization process was used to make the data dimensionless and, thus, to eliminate the influence of different sub-systems on hydrological hazard susceptibility. The higher values of the indicators in this study represent more susceptibility to hazard and, therefore, the following formula was used for the standardization of data,

$$x_i' = \frac{x_i - x_{i(\min)}}{x_{i(\max)} - x_{i(\min)}} \tag{5}$$

where x_i is the original value of indicator i; and $x_{i(\max)}$ and $x_{i(\min)}$ are the maximum and minimum values of the indicator i.

3.2.4. Normalization Using Catastrophe Theory

Catastrophe theory [52] originates from the topology branch of mathematics. The basic purpose of Catastrophe theory is to deal with the phenomena of discontinuity [27,53]. The catastrophe method

uses analytical hierarchy, utility function, and fuzzy evaluation to obtain catastrophe fuzzy membership functions by normalization of the bifurcation set. The dependency of the state variable (index) on control variables (climate indicators) is determined by catastrophic fuzzy membership functions, rather than weights assigned by the users.

In Catastrophe theory, initially, the standardized data are normalized using catastrophe fuzzy mathematics to give the optimal or cleanest data. The multidimensional catastrophe fuzzy membership functions assign values ranging from 0 to 1 to resolve incompatibility of various initial data [52]. There are seven catastrophe models, among which five have one state variable namely, Fold, Cusp, Dovetail, Butterfly, and Wigwam. As the objective of the study is to estimate a single index e.g., HHSI, the catastrophe models having one state variable were considered in this study.

Catastrophe models can handle a maximum of five control variables. Therefore, all the indicators are classified into five classes to show the maximum diversity of data. The Wigwam normalization formula of catastrophe theory was used to derive the catastrophe fuzzy membership function of the indicators as there are five control variables. One state variable represents each sub-system, which is as below:

$$x_a = a^{1/2},\ x_b = b^{1/3},\ x_c = c^{1/4},\ x_d = d^{1/5} \text{ and } x_e = e^{1/6} \quad (6)$$

where a, b, c, d and e are the mean values of four ranges of an indicator and x_a, x_b, x_c, x_d and x_e are the normalized values.

3.2.5. Estimation of Hydrological Hazard Susceptibility Index (HHSI)

The catastrophe theory-based evaluation method was used for the estimation of HHSI from the sub-system indicators mentioned above. The procedure used in the present study for the estimation of HHSI is described below:

1. The system of hydrological hazard susceptibility is divided into four sub-systems namely, COV, PCI, AI and SDR, each of them consists of an evaluation indicator system.
2. The indicator data over the study area are decomposed or classified into a number of levels using Jenks optimization method.
3. The average value of each decomposed or classified data was considered to represent each indicator.
4. Standardized method is used to convert the indicator values to dimensionless numbers in the range of 0 to 1 in order to remove the influence of range and units of different indicators.
5. The catastrophe model for the indicators of the sub-systems is determined based on the levels of evaluation indicators.
6. Catastrophe model is used to estimate the value of fuzzy membership function for normalize evaluation indicator values.
7. The process is repeated to fuzzy membership function values of all indicators of all sub-systems.
8. The average of fuzzy membership function values is estimated as the weight of each sub-system on the hydrological hazard susceptibility system considering that the control variables can compensate each other (complementarity principle).

The fuzzy membership function values are used as rank or importance of each indicator of a subsystem, while the average of the fuzzy membership function values was used as the weight of the sub-system, which defines the importance of the sub-system on the hydrological hazard susceptibility system. Therefore, HHSI was calculated using Equation (7):

$$\text{HHSI} = \frac{COV_w COV_r + PCI_w PCI_r + AI_w AI_r + SDR_w SDR_r}{COV_w + PCI_w + AI_w + SDR_w} \quad (7)$$

where the subscripts, w and r represent weight and rank, respectively. In case of equal weight, all the sub-systems are given a weight equal to 1.

3.2.6. Spatial Mapping

Obtained results in different grid points were used to show the spatial pattern of variables and HHSI to provide a better understanding of the distribution of hydrological hazard susceptibility over the study area. ArcGIS 10.3 provides several ways to display the spatial patterns of an event on the map. In the present study, HHSI values were presented at each grid point using map symbols (points, area fills, color, etc.) of ArcGIS 10.3. Different colors were used to show the magnitude of changes at each grid point.

4. Results and Discussion

4.1. Spatial Distribution of Indicators

In the present study, gridded rainfall and temperature data with a spatial resolution of 0.25° was used. The indicators were estimated for each grid point. The maps showing the spatial distribution of four indicators namely, COV, PCI, AI and SDR are shown in Figure 4.

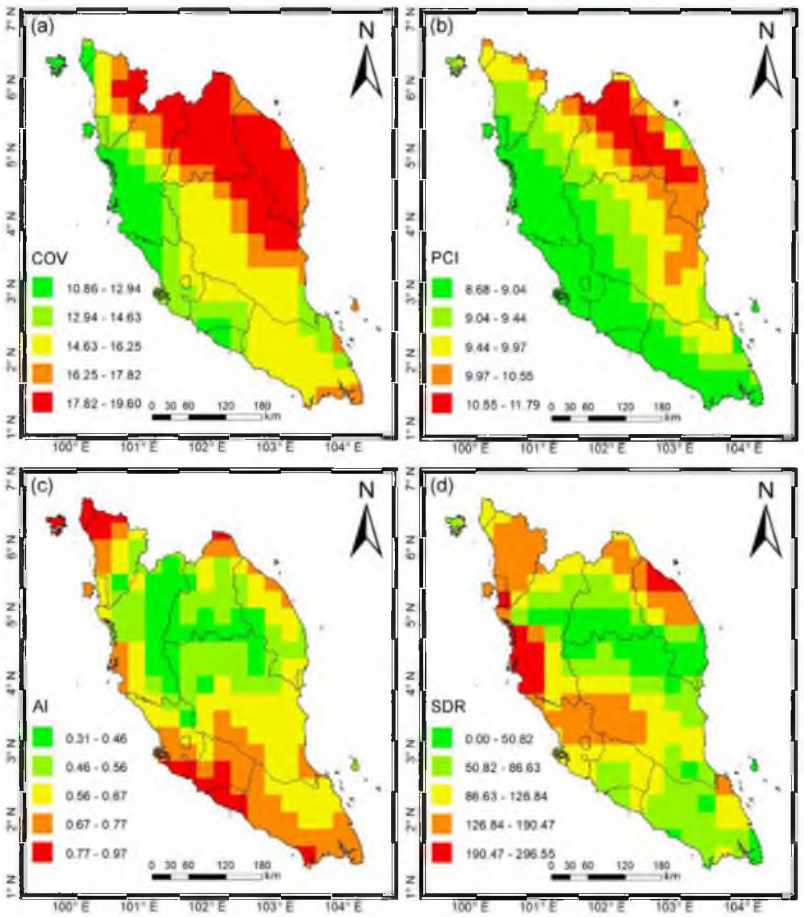

Figure 4. Spatial distribution of indicators over Peninsular Malaysia: (**a**) COV; (**b**) PCI; (**c**) AI; and (**d**) SDR estimated for the period 1948–2010.

4.2. Assignment of Weights to Indicators Using Catastrophe Theory

The value of each indicator was standardized according to Equation (5). After standardization, the raw data was classified into five ranges using Jenks data clustering method and then normalized. The normalized values were obtained from the normalization formula given in Equation (6). For example, the values of the indicators of COV were classified into five classes, 10.86–12.34, 12.34–14.22, 14.22–15.85, 15.85–17.36 and 17.36–19.76 using data clustering method. The mean

values of each range were normalized using equation (6) as, $X_{C1} = 1.0^{1/2} = 1.0$, $X_{C2} = 0.76^{1/3} = 0.91$, $X_{C3} = 0.51^{1/4} = 0.84$, $X_{C4} = 0.28^{1/5} = 0.78$ and $X_{C5} = 0.0^{1/6} = 0.0$. The average of the normalized values was calculated, $(X_{C1} + X_{C2} + X_{C3} + X_{C4} + X_{C5})/5 = 0.71$, which is the weight of the indicator, COV. Similarly applying the same procedure, the weights of PCI, AI and SDR were estimated as 0.73, 0.73 and 0.71, respectively. The estimated values of the fuzzy membership function of different indicators and the weights of the sub-systems are shown in Table 1.

In catastrophe theory, the weight of a sub-system depends on the variance among the mean value of sub-system indicators. It estimates similar weights of two sub-systems when the variabilities of both sub-system indicators are similar. The major advantage of the catastrophe theory-based weighting approach is that it quantifies the real importance of each sub-system according to its indicator values.

Table 1. Estimation of catastrophe fuzzy membership function values of different indicators and the weights of different sub-system used for the estimation of hydrological hazard susceptibility index.

System	Sub-System	Indicators	Average Value	Standardize Value	Normalize Value	Weight
HHSI	COV	10.86–12.34	11.60	1.00	1.00	0.71
		12.34–14.22	13.28	0.76	0.91	
		14.22–15.85	15.03	0.51	0.84	
		15.85–17.36	16.60	0.28	0.78	
		17.36–19.76	18.56	0.00	0.00	
	PCI	8.68–9.04	8.86	1.00	1.00	0.73
		9.04–9.44	9.24	0.84	0.94	
		9.44–9.97	9.70	0.64	0.89	
		9.97–10.55	10.26	0.39	0.83	
		10.55–11.79	11.17	0.00	0.00	
	AI	0.31–0.46	0.38	1.00	1.00	0.71
		0.46–0.56	0.51	0.73	0.90	
		0.56–0.67	0.61	0.52	0.85	
		0.67–0.77	0.72	0.31	0.79	
		0.77–0.97	0.87	0.00	0.00	
	SDR	0–50.82	25.41	1.00	1.00	0.73
		50.82–86.63	68.72	0.80	0.93	
		86.63–126.84	106.74	0.63	0.89	
		126.84–190.47	158.66	0.39	0.83	
		190.47–296.55	243.51	0.00	0.00	

4.3. Estimation of Hydrological Hazard Susceptibility Index

The ranks and weights estimated for COV, PCI, AI and SDR are inserted in Equation (7) to calculate *HHSI* at each grid point. The spatial distribution of HHSI in Peninsular Malaysia is shown in Figure 5. It shows higher susceptibility to hydrological hazards in the NEM region of Peninsular Malaysia. The interiors of the west and the south of the peninsula are found to be less susceptible to hydrological hazards. Furthermore, it was found that coastal regions are more susceptible to hydrological hazards compared to the interior of the peninsula. This matches well in the general conception of the hydrological hazard-prone zone of Peninsular Malaysia [54]. The region receives very high rainfall during NEM and scant rainfall during SWM. Some parts of the study area often suffer flooding mainly due to heavy rainfall during NEM. On the other hand, the longest dry spell is also observed in the region during SWM, particularly in the months of June and July.

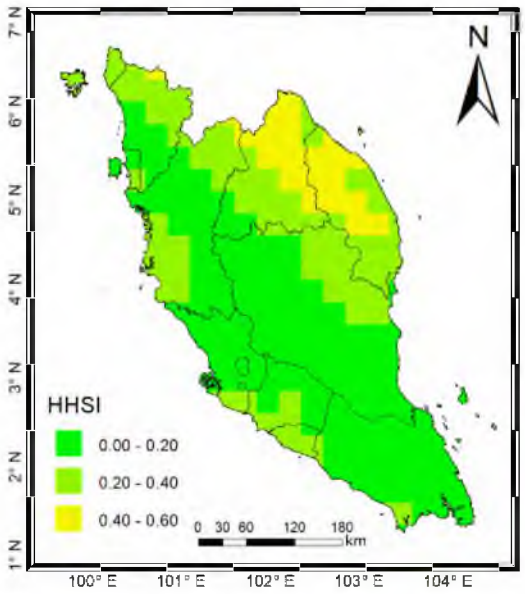

Figure 5. Spatial distribution of hydrological hazard susceptibility in Peninsular Malaysia obtained through integration of hydro-climatic indicators using fuzzy catastrophe method.

The HHSI is also estimated by an assigned equal weight to all sub-systems in Equation (7). The spatial distribution of HHSI using equal weight is shown in Figure 6. It shows a similar pattern of spatial distribution of hydrological hazard susceptibility in Peninsular Malaysia obtained from catastrophe theory. However, the HHSI values obtained from equal weights are found a bit higher compared to those obtained using the catastrophe theory. Figure 6 shows more susceptibility to hydrological hazard in a large area in the northeast region of Peninsular Malaysia. The result indicates that the proposed index can be employed for reasonable assessment of the spatial distribution of hydrological hazard susceptibility through simple calculation by considering the equal influence of all climatic indicators.

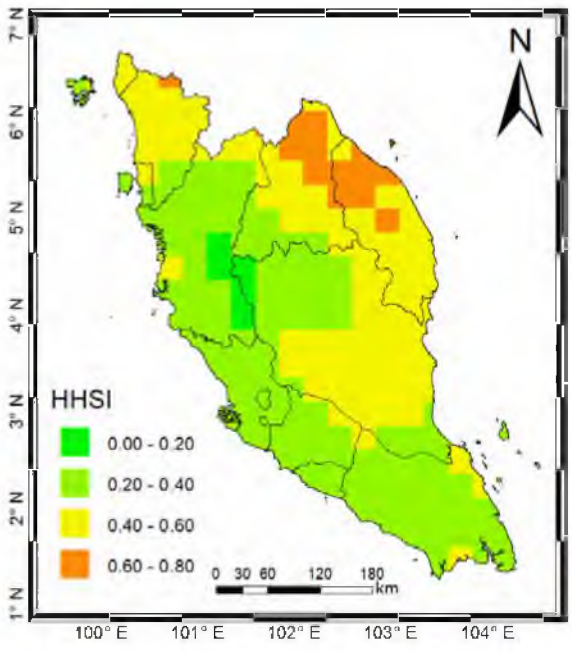

Figure 6. Spatial distribution of hydrological hazard susceptibility in Peninsular Malaysia obtained through integration of hydro-climatic indicators using equal weights.

To understand the causes of higher vulnerability to hydrological hazards in NEM of the peninsula compared to the western part, the indicator values at two grid points, one in the NEM (Kelantan) and another in the west (Melaka) of the peninsula were scrutinized (refer to Figure 1). The indicator values of these two points are presented in the radar chart in Figure 7. The standardized indicator values show less annual and spatial variability and seasonal concentration of rainfall in Melaka compared to Kelantan. The AI values were also found less in Melaka compared to Kelantan.

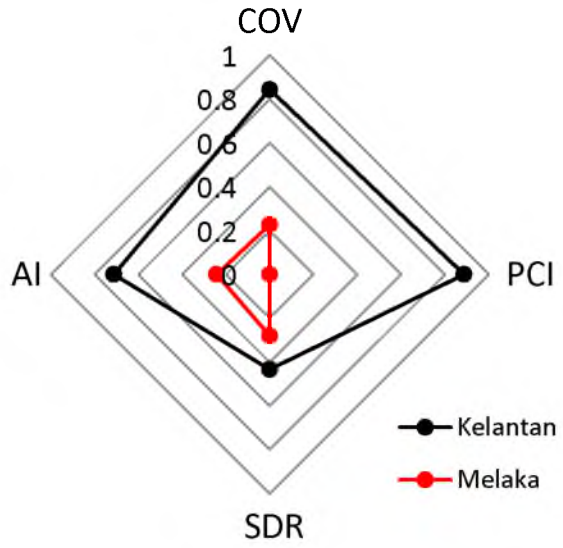

Figure 7. Radar Chart showing the differences in standardized indicator values in Melaka (west coast) and Kelantan (northeast coast).

The annual and seasonal variations of rainfall and AI of those two points were further analyzed to understand the differences in susceptibility to hydrological hazards using PGF data. The seasonal distribution of rainfall in the same two locations is shown in Figure 8. It clearly shows a high concentration of rainfall during NEM in Kelantan compared to Melaka. The amount of rainfall in Melaka in most of the year was found less compared to NEM in Kelantan. The high rainfall during NEM and the comparatively less rainfall in other months have made the region susceptible to floods during NEM and droughts in other months.

The geographic distribution of floods and droughts is not uniform over Peninsular Malaysia. The east coast of Peninsular Malaysia is more prone to hydrological hazards than the west [55]. Floods triggered by heavy rainfall is an almost every year phenomenon in the northeastern coast states of Peninsular Malaysia [56]. It experienced severe floods in 1926, 1967, 1971 and 2014 with catastrophic effects on livelihood and economy [54,57]. Water scarcity due to prolonged dry spells is also a common phenomenon on the northeast coast. Kelantan has experience droughts in 1997, 1998, 2002, 2003, 2005, 2006, 2007, 2009 and 2010 [58,59]. On the other hand, hydrology-related natural hazards are a lot less in Melaka, located on the west coast. The index used and developed in this study was able to reflect the existing spatial distribution of hydrological hazard susceptibility in Peninsular Malaysia. It was able to clearly show the high hydrological hazard susceptibility in Kelantan and the low hydrological hazard susceptibility in Melaka.

The temporal variability of annual rainfall at two locations over the period 1948–2010 is shown in Figure 9. It clearly shows the high annual variability of rainfall in Kelantan compared to Melaka. Rainfall in Kelantan was found to be as high as 4300 mm and as little as 1500 mm in some years compared to the annual average of 3000 mm. On the other hand, rainfall in Melaka was found to be more consistent over the year.

The time series of AI in the same two locations (Figure 10) show higher PET compared to rainfall in Kelantan. The higher PET is responsible for the water scarcity of a region. The spatial variability of

rainfall in Kelantan and Melaka can be assessed from an annual rainfall distribution map of Peninsular Malaysia shown in Figure 2a. The map shows high variability of rainfall in a small region in the NE compared to other parts of the peninsula. The wide heterogeneity of rainfall is also the cause of high susceptibility of hydrological hazard in the region.

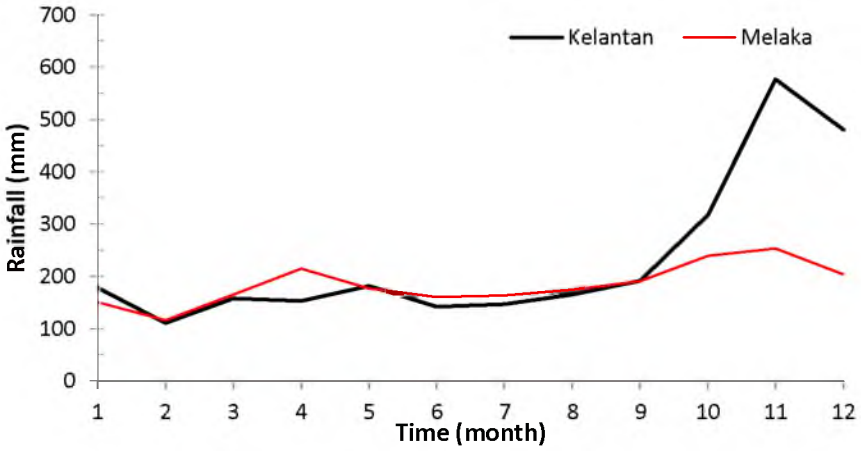

Figure 8. Seasonal distribution of two grid points location in Kelantan and Melaka rainfall estimated for the period 1948–2010.

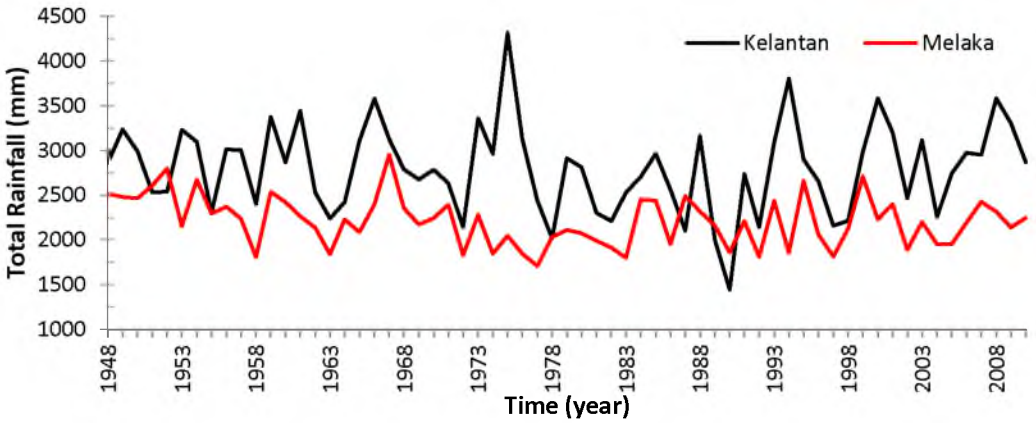

Figure 9. Annual rainfall time series for the period 1948–2010 at two grid points located in Kelantan and Melaka.

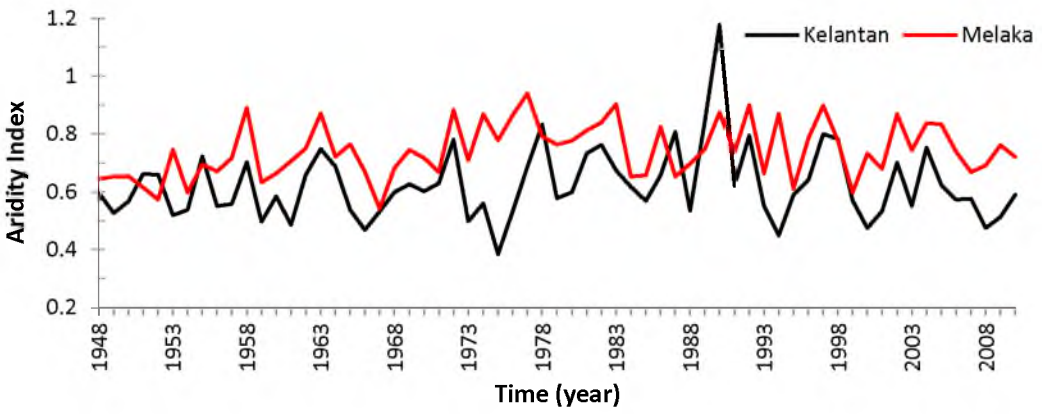

Figure 10. The time series of aridity index for the period 1948-2010 at two grid points located in Kelantan and Melaka.

4.4. Changes in Hydrological Hazard Susceptibility Index

The HHSI is used to assess the changes in geographical distribution of hazard susceptibility in Peninsular Malaysia due to changes in climate. Therefore, HHSI is calculated for every 30-year window between 1950 and 2010. The changes in spatial distribution of HHSI during different periods obtained using catastrophe theory are shown in Figure 11. It shows changes of HHSI in some parts of the peninsula for the recent years. The decrease in HHSI was noticed in the NE of Peninsular Malaysia, which is considered as the most hydrological hazard-prone zone of the peninsula. On the other hand, it was found to increase in the whole southern region of the peninsula.

The equal weight method is also used to assess the changes in geographical distribution of hazard susceptibility. Obtained results are presented in Figure 11, which shows a similar pattern in spatial changes in hydrological hazard in Peninsular Malaysia for both methods.

To understand the causes of the decrease in HHSI, changes in all indicators at all grid points over Peninsular Malaysia were estimated. The changes (%) in COV, PCI, AI and SDR for the recent years (2000–2010) compared to those for the base period 1951–1980 are shown in Figure 12. It shows that rainfall becomes more dependable in the NE of peninsular Malaysia compared to the base period and, therefore, COV has reduced. Some locations on the west coast and the south of the peninsula experienced low increases. The PCI was not found to significantly change in most parts of the peninsula, while both AI and SDR were found to decrease in most parts of the region.

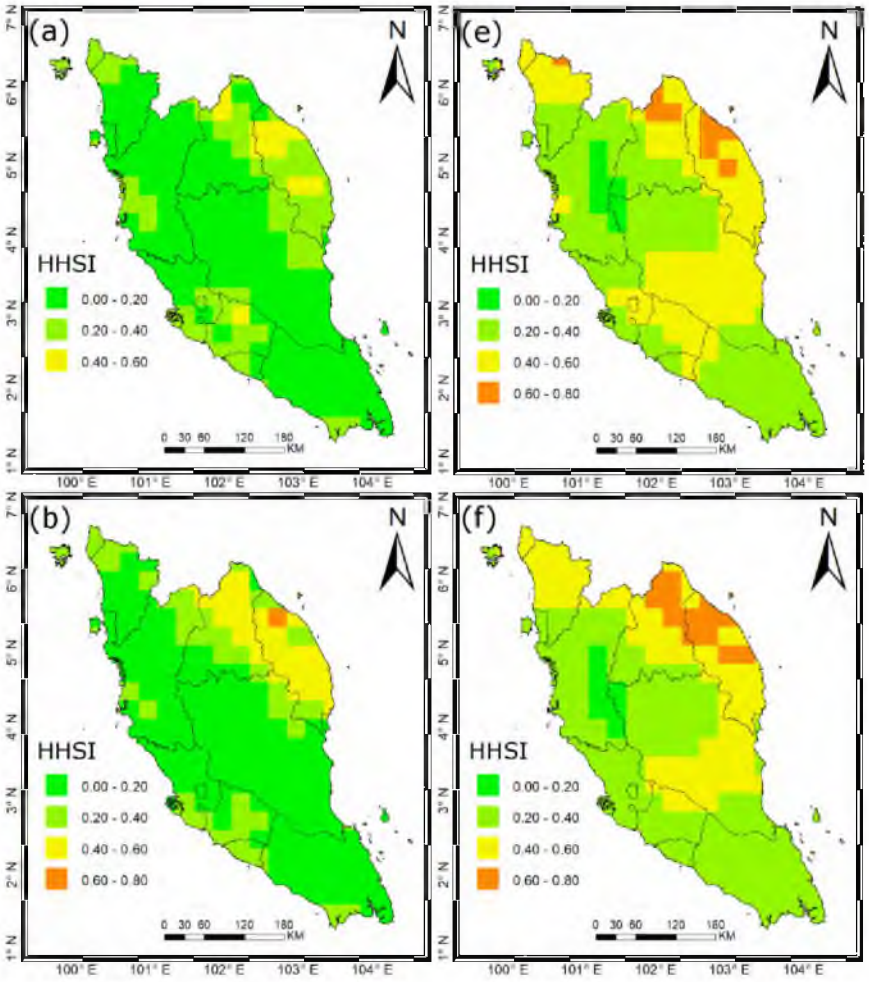

Figure 11. *Cont.*

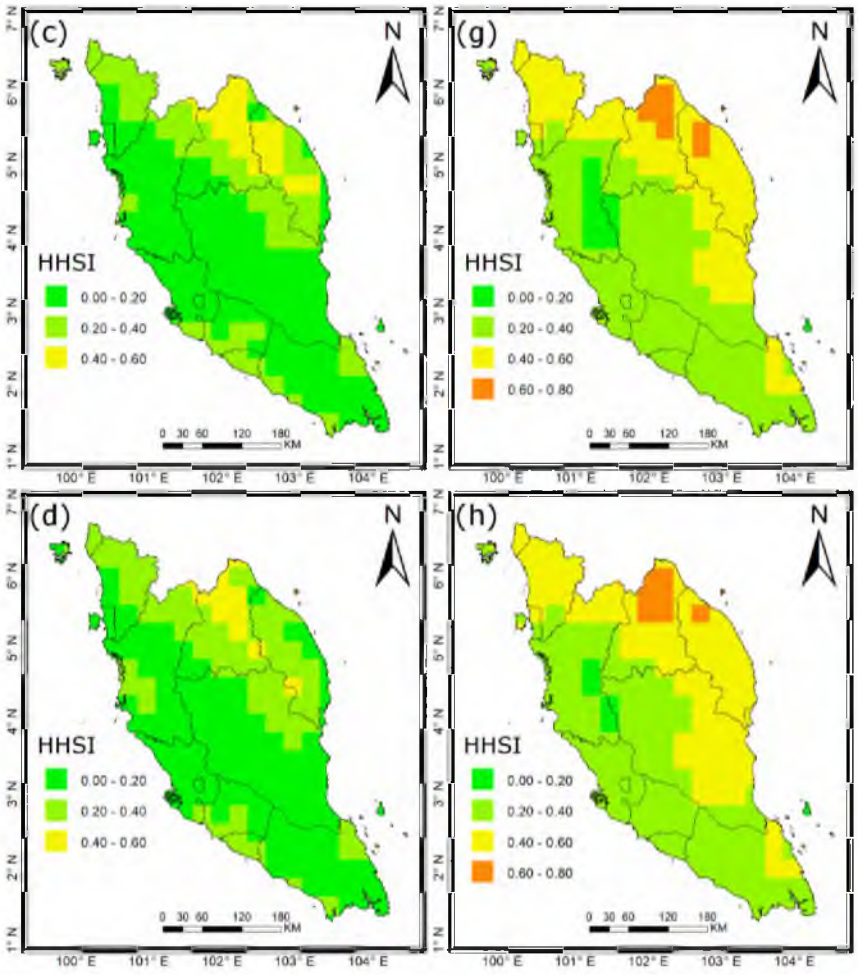

Figure 11. Changes in geographical distribution of hydrological hazard susceptibility using fuzzy catastrophe method (left) in Peninsular Malaysia during different periods: (**a**) 1951–1980; (**b**) 196–1990; (**c**) 197–2000; and (**d**) 198–2010 and using equal weights (right) during (**e**) 195–1980; (**f**) 1961-1990; (**g**) 197–2000; and (**h**) 198–2010.

The variations in individual indicators changed the spatial distribution of HHSI in the peninsula. The changes in susceptibility to hydrological hazards in Peninsular Malaysia in recent years (2000–2010) compared to the base period (1951–1980) are shown in Figure 13. It shows the decrease in hazard susceptibility in the northern part of the peninsula including the NE region, while susceptibility increased in the south. However, the percentage of decrease was in the range of −31.84% and −15.18%, while the increase in the southern part of the peninsula was as high as 21.01%. It has been reported that temperature is increasing and the rainfall pattern is changing in Peninsular Malaysia [55,56]. The present study indicates that changes in rainfall and temperature have overall deteriorated the hydrological hazard susceptibility in Peninsular Malaysia.

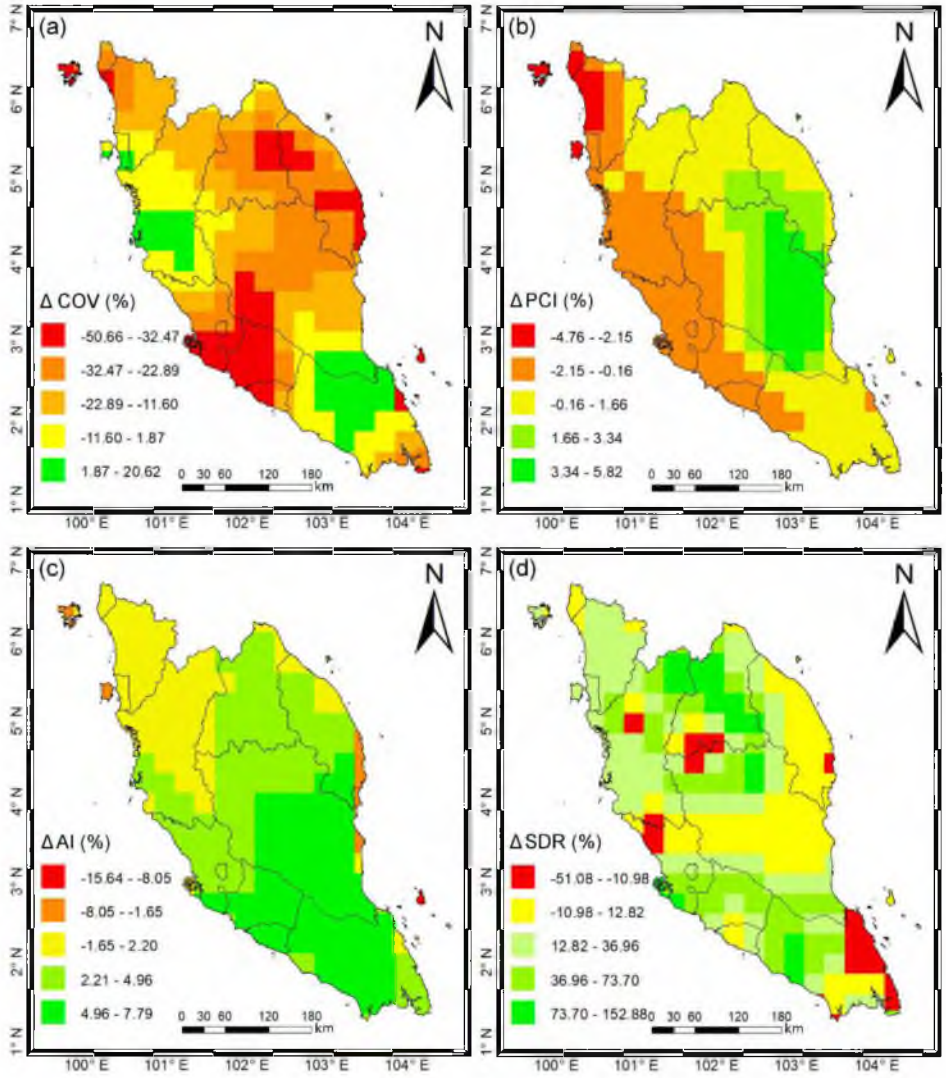

Figure 12. Changes (%) in (**a**) COV; (**b**) PCI; (**c**) AI; and (**d**) SDR in the recent years (2000–2010) compared to the base year (195–1980) in Peninsular Malaysia.

The climate-based index developed in this study can be used for easy computation of hydrological hazard susceptibility from readily available data in any regions. Fuzzy catastrophe theory with data clustering approach is used to reduce subjectivity when estimating the index from multiple numbers of indicators. The application of the hazard susceptibility assessment tool in Peninsular Malaysia showed its capability to map hydrological hazard susceptible zones. The index was also found to assess the recent changes in hazard susceptibility and the factors responsible for those changes. The HHSI, estimated using the equal weight method, is found to provide a similar spatial pattern in hazard susceptibility to that obtained using catastrophe theory, which indicates that simple averaging of the four climatic indicators proposed in this study can be used for fast and easy assessment of hydrological hazard susceptibility in any region. The HHSI developed in this study can be used as a tool for the assessment of the possible impact of climate change on water-related hazards in a region and demarcation of climate change-vulnerable zones. It can also be used to assist policy makers to prioritize adaptation and mitigation measures related to water resource management.

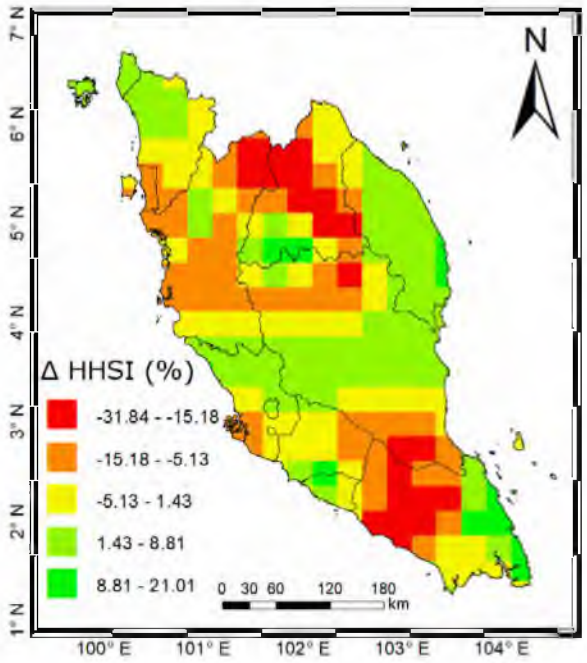

Figure 13. Changes (%) in susceptibility to hydrological hazards in recent years (2000–2010) compared to the base year (1951–1980) in Peninsular Malaysia.

Global warming induced by climate change has caused a sharp rise in temperature and changes in precipitation patterns in most parts of the globe. This has caused an increase in hydrological hazard susceptibility and climate change vulnerability. Assessment of such changes requires assimilation of data from various sources and to analyze data using sophisticated models. The index developed in this study can be used to provide an overall view and preliminary assessment of the climate change impact on hydrological hazard susceptibility. It can be also used to understand the causes of hazard susceptibility, which in turn can help in mitigation planning and future changes in hazard susceptibility using future rainfall and temperature data from general circulation models.

5. Conclusions

Fuzzy catastrophe theory with data clustering approach has been used in this study for the assessment of the geographical distribution of hydrological hazard susceptibility from readily available monthly gridded climate data. The efficacy of the index in the estimation of hydrological hazard susceptibility was assessed through its application in Peninsular Malaysia. The method was found to well construct the spatial distribution of hydrological hazard susceptibility of Peninsular Malaysia. It reliably estimated higher susceptibility of hydrological hazard in the northern part of the east coast and lower susceptibility in the west coast of Peninsular Malaysia. The advantages of the approach developed in this study are: (1) It uses global gridded climate data and, therefore, it can be used in any regions of the world irrespective of availability of data; (2) it uses catastrophe theory to assign weights of different criteria according to the importance of one criterion over others by its inner mechanism and, thus, greatly reduces the subjectivity; (3) the use of natural break algorithm for classification of indicator values further reduces human bias in estimation of hazard index. The proposed method can be used for a more detailed spatial assessment of hydrological hazards with availability of higher spatial resolution climate data in future. Furthermore, study can also be conducted to assess the impacts of climate changes on the spatial and temporal variability of hydrological hazard susceptibility using projected climate under different climate change scenarios.

Author Contributions: M.S.N. and S.S. conceived and designed this study; M.S.N. and K.A. analyzed the data; M.S.N., E.-S.C. and Y.H.S. wrote the paper.

Funding: This work is supported by the Korea Agency for Infrastructure Technology Advancement (KAIA) grant funded by the Ministry of Land, Infrastructure and Transport (Grant 18AWMP-B083066-05). This study was also supported by funding from the National Research Foundation of Korea (NRF 2016R1D1A1B04931844).

Conflicts of Interest: The authors declare no conflict of interest.

References

1. Intergovernmental Panel on Climate Change (IPCC). *Climate Change 2014: Impacts, Adaptation, and Vulnerability*; Part b: Regional Aspects—Contribution of Working Group II to the Fifth Assessment Report of the Intergovernmental Panel on Climate Change; Cambridge University Press: Cambridge, UK, 2014.
2. Shahid, S.; Alamgir, M.; Wang, X.-J.; Eslamian, S. Climate change impacts on and adaptation to groundwater. In *Handbook of Drought and Water Scarcity: Environmental Impacts and Analysis of Drought and Water Scarcity*; CRC Press: Boca Raton, FL, USA, 2017.
3. Eves, C.; Blake, A.; Bryant, L. Assessing the impact of floods and flood legislation on residential property prices. In *International Real Estate Research Symposium (IRES)*; Putra World Trade Centre: Kuala Lumpur, Malaysia, 2010.
4. Brown, C.; Meeks, R.; Hunu, K.; Yu, W. Hydroclimate risk to economic growth in sub-saharan africa. *Clim. Chang.* **2011**, *106*, 621–647. [CrossRef]
5. Shahid, S.; Hadi, P.S.; Xiaojun, W.; Ahmed, S.S.; Anil, M.; Bin, I.T. Impacts and adaptation to climate change in malaysian real estate. *Int. J. Clim. Chang. Strateg. Manag.* **2017**, *9*, 87–103. [CrossRef]
6. Kauko, T.O.M.; Hooimeijer, P.; Hakfoort, J. Capturing housing market segmentation: An alternative approach based on neural network modelling. *Hous. Stud.* **2002**, *17*, 875–894. [CrossRef]
7. Lawrence, P.R.; Meigh, J.; Sullivan, C. *The Water Poverty Index: An International Comparison*; Department of Economics, University of Keele: Staffordshire, UK, 2002.
8. Principles for Responsible Investment (PRI). *Canadian Water Sustainability Index (Cwsi): Project Report*; Policy Research Initiative (PRI): Ottawa, ON, Canada, 2007.
9. Chaves, H.M.L.; Alipaz, S. An integrated indicator based on basin hydrology, environment, life, and policy: The watershed sustainability index. *Water Resour. Manag.* **2007**, *21*, 883–895. [CrossRef]
10. Srdjevic, Z.; Srdjevic, B. An extension of the sustainability index definition in water resources planning and management. *Water Resour. Manag.* **2017**, *31*, 1695–1712. [CrossRef]
11. Hernández-Bedolla, J.; Solera, A.; Paredes-Arquiola, J.; Pedro-Monzonís, M.; Andreu, J.; Sánchez-Quispe, S. The assessment of sustainability indexes and climate change impacts on integrated water resource management. *Water* **2017**, *9*, 213. [CrossRef]
12. Vijith, H. Groundwater potential in the hard rock terrain of western ghats: A case study from kottayam district, kerala using resourcesat (irs-p6) data and gis techniques. *J. Indian Soc. Remote Sens.* **2007**, *35*, 163. [CrossRef]
13. Chowdhury, A.; Jha, M.K.; Chowdary, V.M.; Mal, B.C. Integrated remote sensing and gis-based approach for assessing groundwater potential in west medinipur district, west bengal, india. *Int. J. Remote Sens.* **2009**, *30*, 231–250. [CrossRef]
14. Prasad, R.K.; Mondal, N.C.; Banerjee, P.; Nandakumar, M.V.; Singh, V.S. Deciphering potential groundwater zone in hard rock through the application of gis. *Environ. Geol.* **2008**, *55*, 467–475. [CrossRef]
15. Preeja, K.; Joseph, S.; Thomas, J.; Vijith, H. Identification of groundwater potential zones of a tropical river basin (kerala, india) using remote sensing and gis techniques. *J. Indian Soc. Remote Sens.* **2011**, *39*, 83–94. [CrossRef]
16. Al-Abadi, A.M. Groundwater potential mapping at northeastern wasit and missan governorates, iraq using a data-driven weights of evidence technique in framework of gis. *Environ. Earth Sci.* **2015**, *74*, 1109–1124. [CrossRef]
17. Corsini, A.; Cervi, F.; Ronchetti, F. Weight of evidence and artificial neural networks for potential groundwater spring mapping: An application to the mt. Modino area (northern apennines, italy). *Geomorphology* **2009**, *111*, 79–87. [CrossRef]

18. Ozdemir, A. Using a binary logistic regression method and gis for evaluating and mapping the groundwater spring potential in the sultan mountains (aksehir, turkey). *J. Hydrol.* **2011**, *405*, 123–136. [CrossRef]
19. Lee, S.; Kim, Y.-S.; Oh, H.-J. Application of a weights-of-evidence method and gis to regional groundwater productivity potential mapping. *J. Environ. Manag.* **2012**, *96*, 91–105. [CrossRef] [PubMed]
20. Moghaddam, D.D.; Rezaei, M.; Pourghasemi, H.R.; Pourtaghie, Z.S.; Pradhan, B. Groundwater spring potential mapping using bivariate statistical model and gis in the taleghan watershed, iran. *Arab. J. Geosci.* **2015**, *8*, 913–929. [CrossRef]
21. Pourtaghi, Z.S.; Pourghasemi, H.R. Gis-based groundwater spring potential assessment and mapping in the birjand township, southern khorasan province, iran. *Hydrogeol. J.* **2014**, *22*, 643–662. [CrossRef]
22. Naghibi, S.A.; Pourghasemi, H.R.; Pourtaghi, Z.S.; Rezaei, A. Groundwater qanat potential mapping using frequency ratio and shannon's entropy models in the moghan watershed, iran. *Earth Sci. Inform.* **2015**, *8*, 171–186. [CrossRef]
23. Elmahdy, S.I.; Mohamed, M.M. Probabilistic frequency ratio model for groundwater potential mapping in al jaww plain, uae. *Arab. J. Geosci.* **2015**, *8*, 2405–2416. [CrossRef]
24. Nampak, H.; Pradhan, B.; Manap, M.A. Application of gis based data driven evidential belief function model to predict groundwater potential zonation. *J. Hydrol.* **2014**, *513*, 283–300. [CrossRef]
25. Manap, M.A.; Sulaiman, W.N.A.; Ramli, M.F.; Pradhan, B.; Surip, N. A knowledge-driven gis modeling technique for groundwater potential mapping at the upper langat basin, malaysia. *Arab. J. Geosci.* **2013**, *6*, 1621–1637. [CrossRef]
26. Al-Abadi, A.M.; Shahid, S. A comparison between index of entropy and catastrophe theory methods for mapping groundwater potential in an arid region. *Environ. Monit. Assess.* **2015**, *187*, 576. [CrossRef] [PubMed]
27. Ahmed, K.; Shahid, S.; bin Harun, S.; Ismail, T.; Nawaz, N.; Shamsudin, S. Assessment of groundwater potential zones in an arid region based on catastrophe theory. *Earth Sci. Inform.* **2015**, *8*, 539–549. [CrossRef]
28. Wang, X.-J.; Zhang, J.-Y.; Tong, X.-W.; Shamsuddin, S.; He, R.-M.; Xia, X.-H. Mechanism and comprehensive countermeasure for drought management from the view of catastrophe theory. *Nat. Hazards* **2014**, *71*, 823–835. [CrossRef]
29. Yang, F.; Shao, D.; Xiao, C.; Tan, X. Assessment of urban water security based on catastrophe theory. *Water Sci. Technol.* **2012**, *66*, 487–493. [CrossRef] [PubMed]
30. Al-Abadi, A.M.; Shahid, S.; Al-Ali, A.K. A gis-based integration of catastrophe theory and analytical hierarchy process for mapping flood susceptibility: A case study of teeb area, southern iraq. *Environ. Earth Sci.* **2016**, *75*, 687. [CrossRef]
31. Wang, X.; Zhang, J.; Shahid, S.; Xia, X.; He, R.; Shang, M. Catastrophe theory to assess water security and adaptation strategy in the context of environmental change. *Mitig. Adapt. Strateg. Glob. Chang.* **2014**, *19*, 463–477.
32. Thornthwaite, C.W. An approach toward a rational classification of climate. *Geogr. Rev.* **1948**, *38*, 55–94. [CrossRef]
33. Ahmed, K.; Chung, E.-S.; Song, J.-Y.; Shahid, S. Effective design and planning specification of low impact development practices using water management analysis module (wmam): Case of malaysia. *Water* **2017**, *9*, 173. [CrossRef]
34. Sheffield, J.; Goteti, G.; Wood, E.F. Development of a 50-year high-resolution global dataset of meteorological forcings for land surface modeling. *J. Clim.* **2006**, *19*, 3088–3111. [CrossRef]
35. Zhu, Y.; Lin, Z.; Zhao, Y.; Li, H.; He, F.; Zhai, J.; Wang, L.; Wang, Q. Flood simulations and uncertainty analysis for the pearl river basin using the coupled land surface and hydrological model system. *Water* **2017**, *9*, 391. [CrossRef]
36. Aich, V.; Akhundzadah, N.; Knuerr, A.; Khoshbeen, A.; Hattermann, F.; Paeth, H.; Scanlon, A.; Paton, E. Climate change in afghanistan deduced from reanalysis and coordinated regional climate downscaling experiment (cordex)—South asia simulations. *Climate* **2017**, *5*, 38. [CrossRef]
37. Aadhar, S.; Mishra, V. High-resolution near real-time drought monitoring in south asia. *Sci. Data* **2017**, *4*, 170145. [CrossRef] [PubMed]
38. Wu, C.; Hu, B.X.; Huang, G.; Zhang, H. Effects of climate and terrestrial storage on temporal variability of actual evapotranspiration. *J. Hydrol.* **2017**, *549*, 388–403. [CrossRef]

39. Nashwan, M.S.; Shahid, S.; Abd Rahim, N. Unidirectional trends in annual and seasonal climate and extremes in egypt. *Theor. Appl. Climatol.* **2018**. [CrossRef]
40. Pour, S.H.; Harun, S.B.; Shahid, S. Genetic programming for the downscaling of extreme rainfall events on the east coast of peninsular malaysia. *Atmosphere* **2014**, *5*, 914–936. [CrossRef]
41. Salman, S.A.; Shahid, S.; Ismail, T.; Chung, E.-S.; Al-Abadi, A.M. Long-term trends in daily temperature extremes in iraq. *Atmos. Res.* **2017**, *198*, 97–107. [CrossRef]
42. Shahid, S. Recent trends in the climate of bangladesh. *Clim. Res.* **2010**, *42*, 185–193. [CrossRef]
43. Yli-Viikari, A.; Hietala-Koivu, R.; Huusela-Veistola, E.; Hyvönen, T.; Perälä, P.; Turtola, E. Evaluating agri-environmental indicators (aeis)—Use and limitations of international indicators at national level. *Ecol. Indic.* **2007**, *7*, 150–163. [CrossRef]
44. Niemeijer, D.; de Groot, R.S. A conceptual framework for selecting environmental indicator sets. *Ecol. Indic.* **2008**, *8*, 14–25. [CrossRef]
45. Lin, T.; Lin, J.-Y.; Cui, S.-H.; Cameron, S. Using a network framework to quantitatively select ecological indicators. *Ecol. Indic.* **2009**, *9*, 1114–1120. [CrossRef]
46. Elle, M.; Dammann, S.; Lentsch, J.; Hansen, K. Learning from the social construction of environmental indicators: From the retrospective to the pro-active use of scot in technology development. *Build. Environ.* **2010**, *45*, 135–142. [CrossRef]
47. Ahmed, K.; Shahid, S.; Harun, S.B.; Wang, X.-J. Characterization of seasonal droughts in balochistan province, pakistan. *Stoch. Environ. Res. Risk Assess.* **2016**, *30*, 747–762. [CrossRef]
48. Oliver, J.E. Monthly precipitation distribution: A comparative index. *Prof. Geogr.* **1980**, *32*, 300–309. [CrossRef]
49. Shahid, S. Spatio-temporal variability of rainfall over Bangladesh during the time period 1969–2003. *Asia Pac. J. Atmos. Sci.* **2009**, *45*, 375–389.
50. Liu, Y.; Yan, J.; Cen, M. The relationship between precipitation heterogeneity and meteorological drought/flood in china. *J. Meteorol. Res.* **2016**, *30*, 758–770. [CrossRef]
51. Jenks, G.F. The data model concept in statistical mapping. *Int. Yearb. Cartogr.* **1967**, *7*, 186–190.
52. Wang, W.; Liu, S.; Zhang, S.; Chen, J. Assessment of a model of pollution disaster in near-shore coastal waters based on catastrophe theory. *Ecol. Model.* **2011**, *222*, 307–312. [CrossRef]
53. Ahammed, S.; Chung, E.-S.; Shahid, S. Parametric assessment of pre-monsoon agricultural water scarcity in bangladesh. *Sustainability* **2018**, *10*, 819. [CrossRef]
54. Nashwan, M.S.; Ismail, T.; Ahmed, K. Flood susceptibility assessment in kelantan river basin using copula. *Int. J. Eng. Technol.* **2018**, *7*, 584–590.
55. Yusuf, A.A.; Francisco, H. *Climate change vulnerability mapping for Southeast Asia*; Economy and Environment Program for Southeast Asia (EEPSEA): Singapore, 2009; p. 32.
56. Mayowa, O.O.; Pour, S.H.; Shahid, S.; Mohsenipour, M.; Harun, S.B.; Heryansyah, A.; Ismail, T. Trends in rainfall and rainfall-related extremes in the east coast of peninsular malaysia. *J. Earth Syst. Sci.* **2015**, *124*, 1609–1622. [CrossRef]
57. Shakirah, J.A.; Sidek, L.; Hidayah, B.; Nazirul, M.; Jajarmizadeh, M.; Ros, F.; Roseli, Z. A review on flood events for kelantan river watershed in malaysia for last decade (2001–2010). In *IOP Conference Series: Earth and Environmental Science*; IOP Publishing: Bristol, UK, 2016.
58. Hashim, M.; Reba, N.M.; Nadzri, M.I.; Pour, A.B.; Mahmud, M.R.; Mohd Yusoff, A.R.; Ali, M.I.; Jaw, S.; Hossain, M.S. Satellite-based run-off model for monitoring drought in peninsular malaysia. *Remote Sens.* **2016**, *8*, 633. [CrossRef]
59. Tan, M.L.; Tan, K.C.; Chua, V.P.; Chan, N.W. Evaluation of trmm product for monitoring drought in the kelantan river basin, malaysia. *Water* **2017**, *9*, 57. [CrossRef]